

Research Article

Assessment of Severe Accident Depressurization Valve Activation Strategy for Chinese Improved 1000 MWe PWR

Ge Shao, Lili Tong, and Xuewu Cao

School of Mechanical Engineering, Shanghai Jiao Tong University, 800 Dong Chuan Road, Shanghai 200240, China

Correspondence should be addressed to Lili Tong; lltong@sjtu.edu.cn

Received 24 July 2013; Accepted 18 November 2013

Academic Editor: Bing Li

Copyright © 2013 Ge Shao et al. This is an open access article distributed under the Creative Commons Attribution License, which permits unrestricted use, distribution, and reproduction in any medium, provided the original work is properly cited.

To prevent HPME and DCH, SADV is proposed to be added to the pressurizer for Chinese improved 1000 MWe PWR NPP with the reference of EPR design. Rapid depressurization capability is assessed using the mechanical analytical code. Three typical severe accident sequences of TMLB, SBLOCA, and LOFW are selected. It shows that with activation of the SADV the RCS pressure is low enough to prevent HPME and DCH. Natural circulation at upper RPV and hot leg is considered for the rapid depressurization capacity analysis. The result shows that natural circulation phenomenon results in heat transfer from the core to the pipes in RCS which may cause the creep rupture of pipes in RCS and delays the severe accident progression. Different SADV valve areas are investigated to the influence of depressurization of RCS. Analysis shows that the introduction of SADV with right valve area will delay progression of core degradation to RPV failure. Valve area is to be optimized since smaller SADV area will reduce its effect and too large valve area will lead to excessive loss of water inventory in RCS and makes core degradation progression to RPV failure faster without additional core cooling water sources.

1. Introduction

In severe accidents, the reactor core is damaged and the molten core can relocate to the lower head of the reactor pressure vessel (RPV) while the pressure in the reactor coolant system (RCS) remains relatively high. With the failure of the lower head under these conditions, the molten core material is ejected to the cavity of the reactor vessel, which is generally called high pressure melt ejection (HPME). Furthermore, the temperature and pressure of the containment atmosphere will increase rapidly, which is generally called direct containment heating (DCH) [1, 2]. DCH could induce the containment atmosphere pressure and temperature increase rapidly, which would challenge the structure integrity of the containment [3]. It is necessary to ensure depressurization before primary system failure by a hardware modification or a procedural measure as prevention of HPME and DCH [4].

Safety Depressurization Systems (SDS) are adopted to enable feed and bleed operation to mitigate severe accidents for advanced light water reactors, such as ABB-CE System 80+, and the Korean standard nuclear power plants of Yonggwang 3 and 4 and Ulchin 3 and 4 [5], Korean Optimized

Power Reactor (OPR) 1000 [6]. In Chinese 600 MWe PWR NPP, the extended function of the existing safety valves is planned to implement the intentional RCS depressurization as one severe accident management strategy. According to the previous research, high temperature gases during the depressurization process may cause failure of the existing safety valves [7]. To secure depressurization of the RCS during severe accident conditions, the two regulating valves of the relief system have been modified in 1999 for Switzerland PWR to keep the valves open with the help of a nitrogen supply or a water supply from outside of the containment [8]. In EPR design, two redundant dedicated severe accident depressurization valves (SADVs) are added to the pressurizer to implement rapid depressurization strategy during severe accidents [9]. The valves are designed and qualified to be able to remain open in severe accident conditions.

With the reference of EPR design, SADV is proposed to be installed on top of the pressurizer in Chinese improved PWR and the area of SADV is 0.0048 m^2 . The Chinese improved PWR has been developed by incorporating the latest technologies and the experiences in construction and operation gained from previous nuclear power plants. The

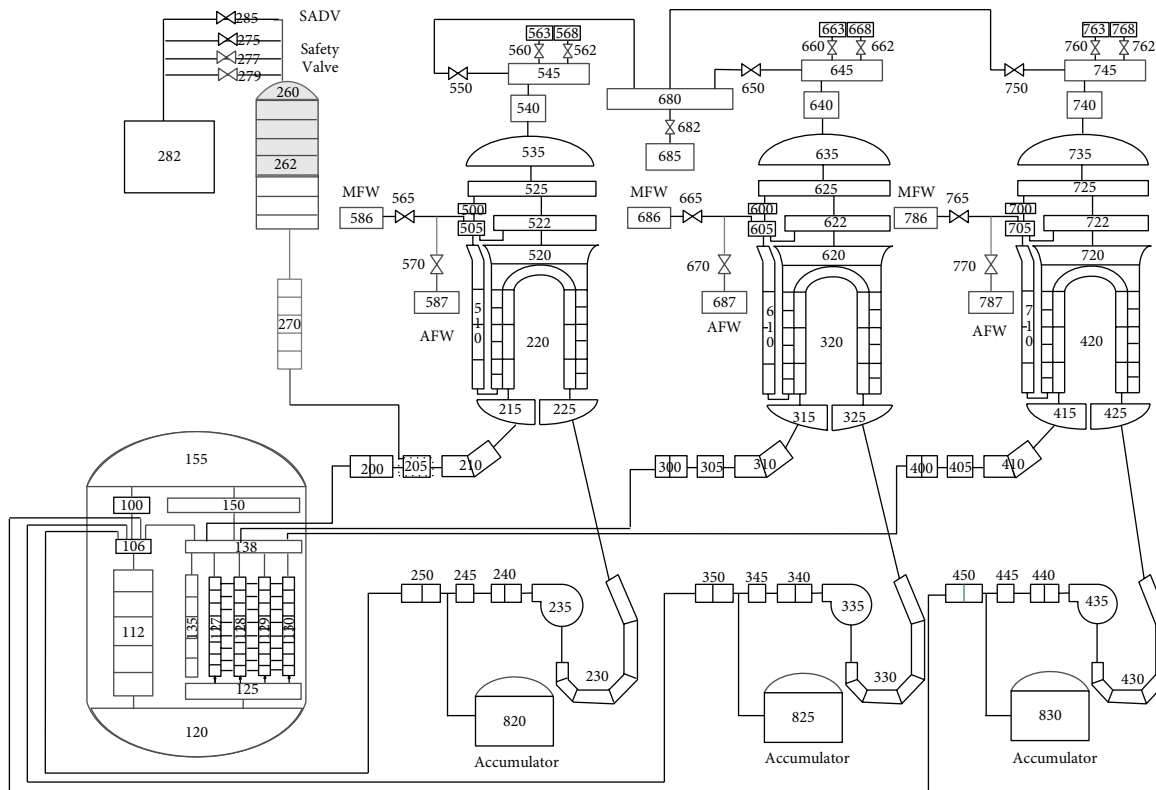


FIGURE 1: Node of plant model.

design features are a three-loop RCS design and a 1000 MWe power level with some modifications for severe accidents prevention and mitigation. In this paper, thermal hydraulic analysis using mechanical safety analytical code is performed for three selected high pressure sequences to investigate the feasibility of rapid depressurization strategy by SADV activation.

2. Plant Model Description

Chinese Improved PWR is modeled by the mechanical safety analytical code, which is based on a nonhomogeneous and nonequilibrium model of two-phase system that is solved by partially implicit numerical scheme. It employs comprehensive six-equation approach that minimizes the necessity of empirical correlations.

The node of plant model includes three loops of primary system, secondary loop, and engineered safety facility as in Figure 1. The RPV, three hot legs, three steam generators (SGs), three intermediate legs, three reactor coolant pumps (RCPs), and three cold legs are modeled for primary system. The reactor core is simulated as four channels to evaluate its thermal hydraulic behavior in detail and each channel is composed of 8 axial volumes. Node 135 represents the core bypass. One surge line and one pressurizer are attached to one of the hot legs. Three accumulators are connected to the cold legs, respectively. The SADV is represented by node 285 and three pressurizer safety valves are represented by nodes 275, 277, and 279. Node 282 represents the containment.

The steam generator secondary side consists of a cylindrical shell, a downcomer through which the main feedwater or auxiliary feedwater is supplied, a separator, and a steam dome. Main steam safety valves, relief valves, and a main steam line isolation valve are also modeled. The turbine is modeled as time-dependent volumes by node 685.

3. Accident Sequence Analysis

According to the PSA results of the reference PWR and the criterion for selecting important severe accident sequences in 10 CFR 50.54(f) [10], three representational accident sequences as TMLB', SBLOCA, and LOFW are selected for the rapid depressurization assessment. These accident scenarios have large contribution to the core damage frequency (CDF) and may cause high pressure core melt. TMLB' sequences are the station black out accident with failure of turbine-driven auxiliary feedwater pump which means total loss of auxiliary feedwater [11]. For SBLOCA, the break is assumed to locate at one cold leg with the equivalent diameter of 12.7 mm. The following assumptions are made for the selected three scenarios.

- (i) High-pressure safety injection (HPSI) system are low-pressure safety injection (LPSI) system are assumed to be unavailable.
- (ii) Accumulators are available.

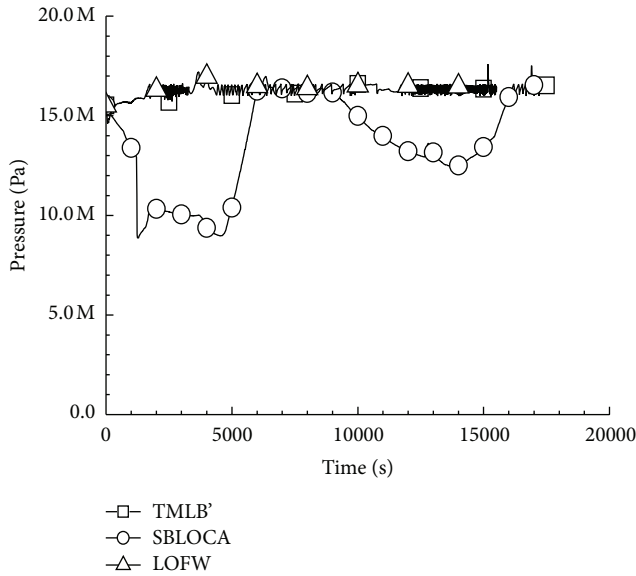


FIGURE 2: RCS pressure without activation of SADV.

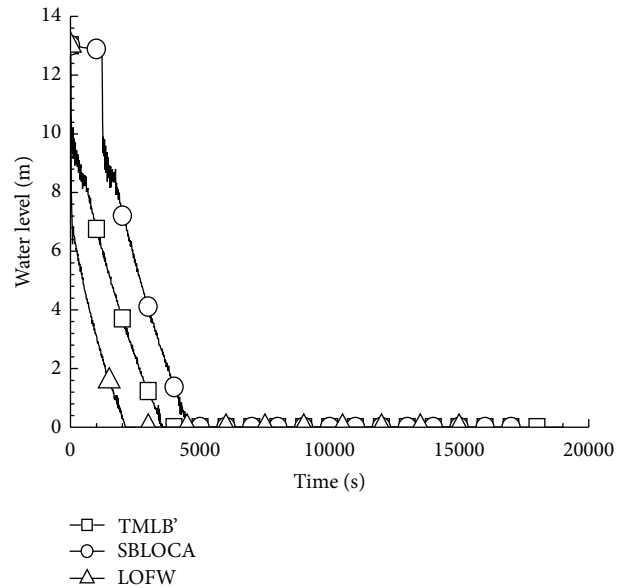


FIGURE 3: Secondary water level of SG without activation of SADV.

(iii) Auxiliary feedwater (AFW) systems are assumed to be unavailable.

(iv) The RCS pipe failure is not considered.

3.1. Accident Scenarios without SADV Activation. For TMLB' scenario, reactor scrams at 0.0 s followed by coastdown of the RCPs, loss of main feed water, and closure of the main steam isolation valves. The RCS pressure decreases at 0.0 s due to the reactor scram (see Figure 2). Then the secondary sides of SGs become empty at 3500 s due to the unavailability of AFW (see Figure 3). The decay heat of the reactor core cannot be removed by the SGs, so the RCS pressure rises up and fluctuates around the setpoint of pressurizer safety valves. Because the HPSI is assumed to be unavailable, the water level of RPV begins to drop with large amount of coolant loss through the safety valves and the reactor core begins to uncover at 5910 s (see Figure 4). The core temperature rises rapidly and the core starts to melt at 8430 s (see Figure 5). Eventually core melts down to the lower head of RPV.

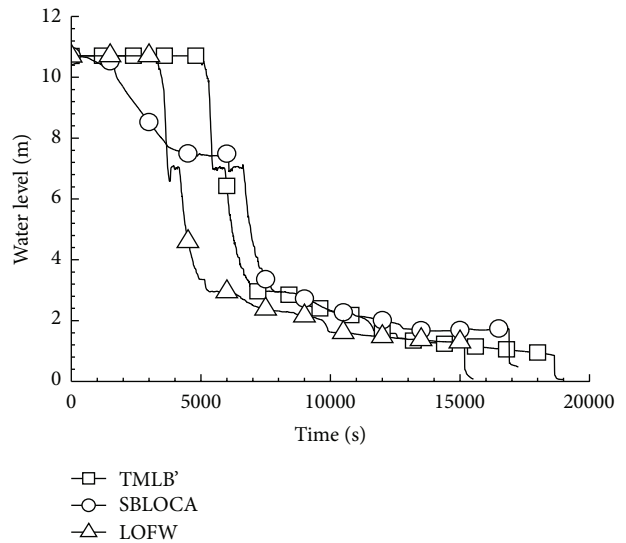


FIGURE 4: Water level of RPV without activation of SADV.

For SBLOCA scenario, the RCS pressure decreases due to the occurrence of the cold leg break (see Figure 2). The reactor scrams at 1220 because the low pressure setpoint of pressurizer is satisfied. The SGs dry up at 4620 due to the loss of AFW (see Figure 3). Then the RCS pressure rises up and fluctuates around the setpoint of pressurizer safety valves. With large amount of coolant loss through the safety valves and the break, reactor core begins to uncover at 6630 s (see Figure 4). The core temperature rises rapidly and the core starts to melt at 8950 s (see Figure 5). Finally core melts down to the lower head of RPV.

the lower head of RPV fails due to creep rupture, the RCS pressure is 16.5 MPa for three selected accidents (see Table 1).

For LOFW scenario, the accident progression is similar to the TMLB' scenario but faster due to the delayed reactor scram. The delay in reactor trip increases the energy stored inside RCS and accelerates the accident progression. When

3.2. Accident Scenarios with SADV Activation. If operators open SADV manually when the core exit temperature exceeds 650°C according to the severe accident management guideline (SAMG) for the three selected accidents, the RCS pressure will drop (see Figure 6) because large quantity of coolant is lost through the SADV (see Figure 7). Accumulators will be activated when the RCS pressure reaches the setpoint (see Figure 8), and water level in RPV will rise up due to the accumulators injection (see Figure 9). When the accumulators are empty, the core is uncovered and ultimately melts down. However, the time when the core starts to melt

TABLE 1: Progressions of the three accident sequences.

Progression (s)	Without SADV activation			With SADV activation		
	TMLB'	SBLOCA	LOFW	TMLB'	SBLOCA	LOFW
Start of accident	0.0	0.0	0.0	0.0	0.0	0.0
Reactor shutdown	0.0	1220	20	0.0	1220	20
Opening SADV manually	/	/	/	7410	8100	5630
Accumulator activation	/	/	/	7410	8100	5630
Start of core melt	8430	8950	6470	12450	12610	10020
Lower head of RPV fails	18990	17250	15520	20100	21850	19050
RCS pressure when lower head of RPV fails/MPa	16.5	16.5	16.5	0.55	0.26	0.31

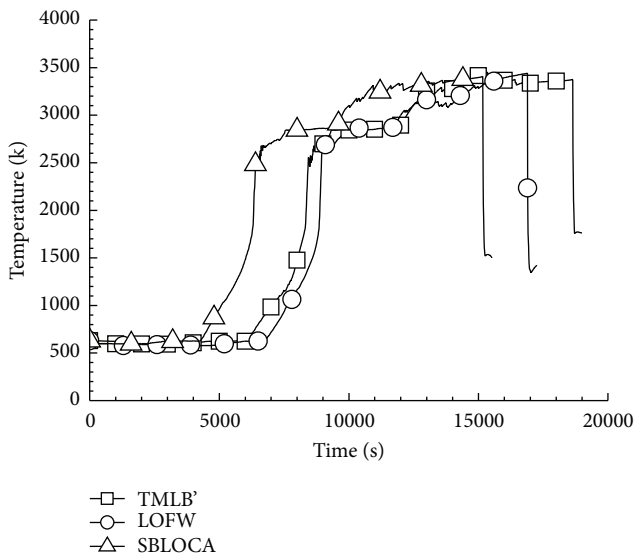


FIGURE 5: Highest core temperature without activation of SADV.

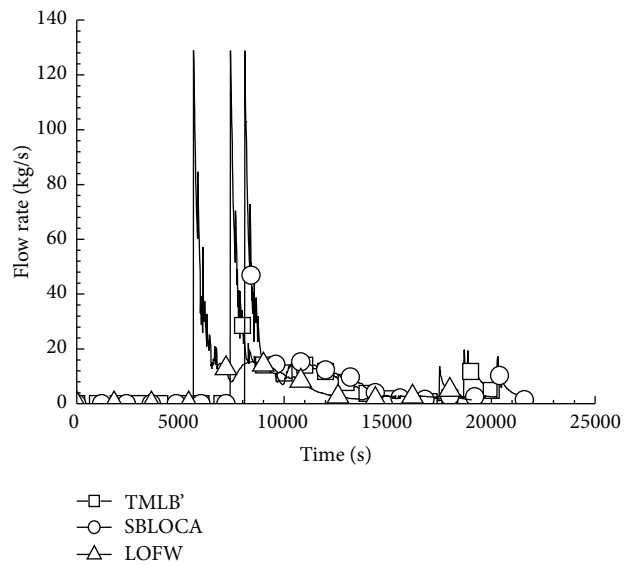


FIGURE 7: Flow rate through SADV with activation of SADV.

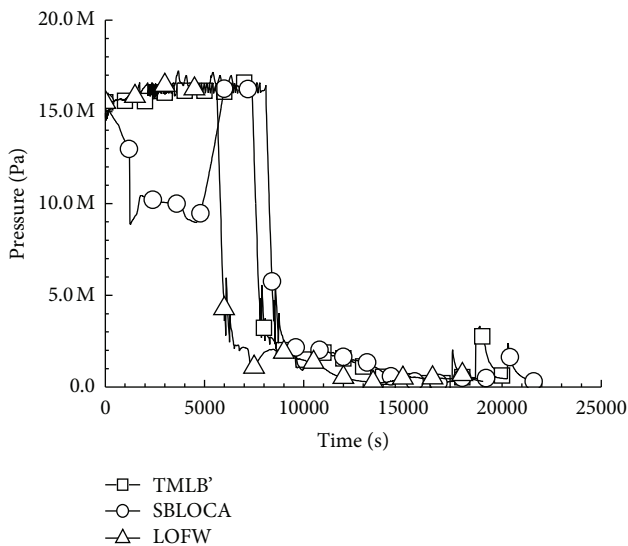


FIGURE 6: RCS pressure with activation of SADV.

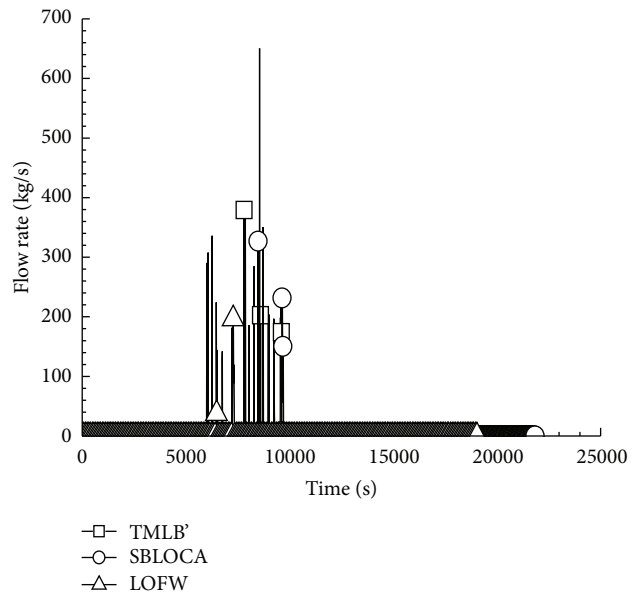


FIGURE 8: Flow rate of accumulator with activation of SADV.

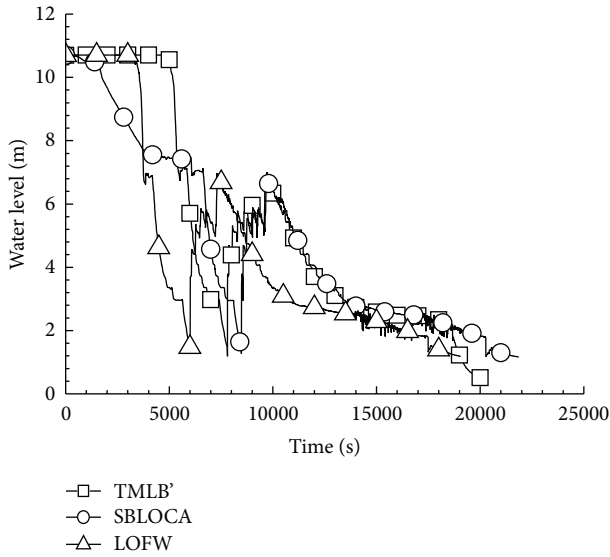


FIGURE 9: Water level of RPV with activation of SADV.

TABLE 2: Comparison of RCS depressurization progression for TMLB' accident.

	Without natural circulation	With natural circulation
Progression (s)		
Start of accident	0.0	0.0
Reactor shutdown	0.0	0.0
Opening SADV manually	7410	8320
Accumulator activation	7800	8580
Start of core melt	12450	15010
Lower head of PRV fails	20100	21945
RCS pressure when lower head of RPV fails/MPa	0.55	0.28

and lower head of RPV fails is delayed by the activation of SADV and the injection of the accumulators (see Table 1).

NUREG-1150 mentions that when the RCS-to-containment pressure difference is less than 1.38 MPa when lower head of RPV fails, the HPME and DCH can be prevented effectively [12]. This criterion is used in the assessment of rapid depressurization. Without activation of SADV, the RCS pressure is 16.5 MPa when lower head of RPV fails. HPME and DCH may happen and cause damage to the integrity of containment. If operators open SADV manually according to SAMG, the RCS pressure is decreased and the values of the three typical sequences at the time of lower head of PRV failure are 0.55 MPa, 0.26 MPa, and 0.31 MPa, respectively, which is much lower than 1.38 MPa, showing that the HPME and DCH can be prevented effectively.

4. Analysis of Uncertainties

4.1. Natural Circulation. After the hot legs have been voided and prior to the loop sealclearing, a countercurrent natural circulation among the reactor vessel, hot legs, and steam generator U-tubes may develop. Superheated vapor enters the top of the hot leg displacing saturated vapor, which then flows back to the reactor vessel along the bottom of the hot leg. When hotter vapor enters the steam generator inlet plenum, it will rise toward the steam generator U-tubes. Vapor enters some of the tubes, displacing cooler steam that was in the tubes. Cooler vapor enters the outlet plenum and then reenters other steam generator tubes, forcing vapor into the inlet plenum. A density gradient is thus established between the tubes which supports the natural circulation. Similarly, in-vessel natural circulation may happen when the core is uncovered and vapor density gradient is established because of the temperature difference. The hot vapor rises to the upper plenum and is cooled by the internal structures. Then vapor flows back to the core where it is reheated and the process is repeated. To simulate natural circulation phenomena, RPV and hot legs model are renodalized (see Figures 10 and 11) because countercurrent flow of a single fluid cannot be calculated in a single control volume. Nodes 131–134, 141–144, 151–154, and 161–164 represent the vapor flow path from core to the upper plenum, respectively. Multiple junctions are added between them to simulate the crossflow. Nodes 181–184 represent the vapor flow path from the upper plenum to core. Nodes 205 and 206 represent the split hot leg segment to the surge line. Nodes 210 and 211 represent the segment to the steam generator inlet plenum. The top pipe carries the hot vapor leaving the upper plenum and the bottom pipe carries the cooler vapor back to the upper plenum. The steam generator inlet plenum is split into 3 control volumes to simulate the steam generator inlet plenum mixing. Node 214 represents the unmixed hot flow entering the plenum from the top hot leg, node 215 represents the mixing volume, and node 216 represents the unmixed cold flow returning from the cold steam generator tubes and flowing toward RPV via the lower portion of the hot leg. Node 220 represents 35% of the SG tubes which carry the hot fluid to the SG outlet plenum and node 221 represents 65% of the tubes which carry the cooler fluid back to the inlet plenum. This proportion is based on the Westinghouse natural circulation experiments [13].

The establishment of natural circulation and the accompanying exchange of thermal energy from the core to the upper plenum and coolant loop internals may induce failure in the RCS before vessel failure is reached [14]. As a result of enhanced cooling of the core by recirculation steam from cooler regions, the onset of core damage would be delayed. This is further enhanced by the mass exchange that will occur between the upper plenum and SGs. A part of the core heat is transported to ex-core region by the natural circulation. Table 2 is the comparison of RCS depressurization progression for TMLB' accident between the case with considering natural circulation and the case without considering

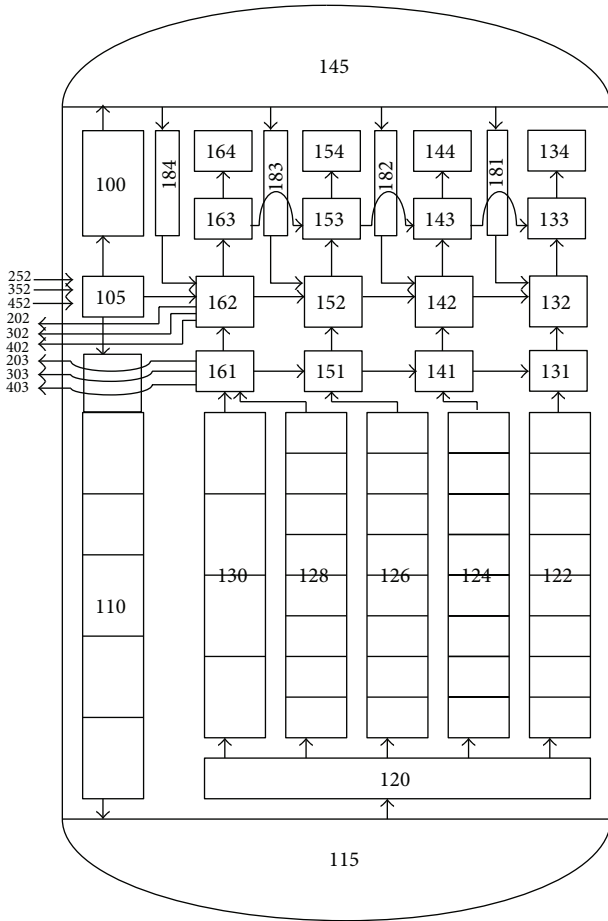


FIGURE 10: Nodalization of in-vessel natural circulation model.

natural circulation. The time of the whole accident progression is delayed due to the natural circulation phenomena. The pressure of RCS when lower head of RPV fails is even lower with natural circulation.

Without SADV activation, the temperature of the hottest part of hot leg given by the first node nearest the RPV in the loop with the pressurizer increases gradually (see Figure 12), and the hot leg fails at 11470 s. The steam produced by accumulator water injection explains the quick reduction for hot leg temperature after SADV activation (see Figure 12). Afterward the natural circulation is arrested by the forced flow from the vessel to the pressurizer, and it is not reestablished after discharge because SADV keeps open. When accumulators are empty, core heats up again and generates hot gas flowing out of the upper plenum to the pressurizer which result that in the hot legs increases slowly. Without SADV activation, the temperature of SG tube increases gradually (see Figure 13) due to the natural circulation, and the SG tube fails at 12570 s. The SG tube temperature decreases when SADV is activated (see Figure 13) because the natural circulation is arrested by the forced flow from the vessel to the pressurizer. The SG tube creep rupture can be avoided by the SADV activation.

Although the creep rupture of pipe in RCS is helpful to reduce the RCS pressure, it is an uncertain method to

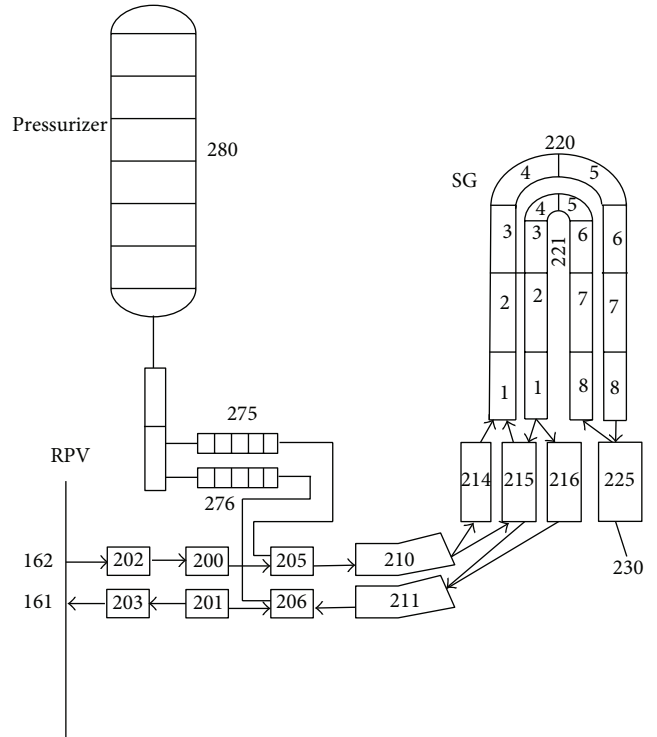


FIGURE 11: Nodalization of hot leg natural circulation model.

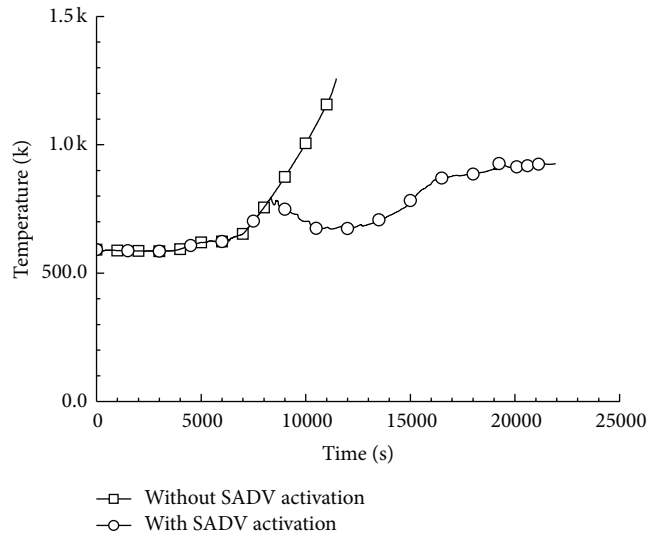


FIGURE 12: Wall temperature of hot leg.

depressurize the RCS. The timing and size of RCS pipe failure is strongly affected by uncertainties in the heat transfer characteristics of the core, the amount of heat transferred to the components in the flow path, and the heat and structural characteristics of the pipes. Thus, the RCS pipe failure is not considered in the analysis of intentional depressurization strategies.

4.2. SADV Valve Area. The discharge capacity is dependent on the SADV valve area which has impacts on the depressurization rate. Several SADV valve areas are chosen for

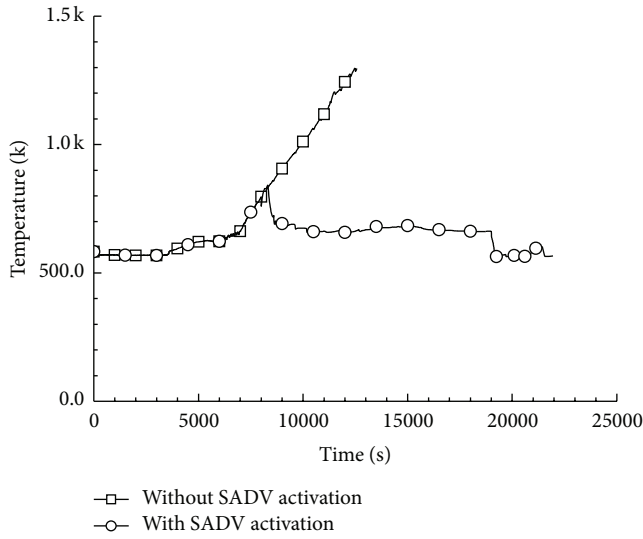


FIGURE 13: Wall temperature of SG tube.

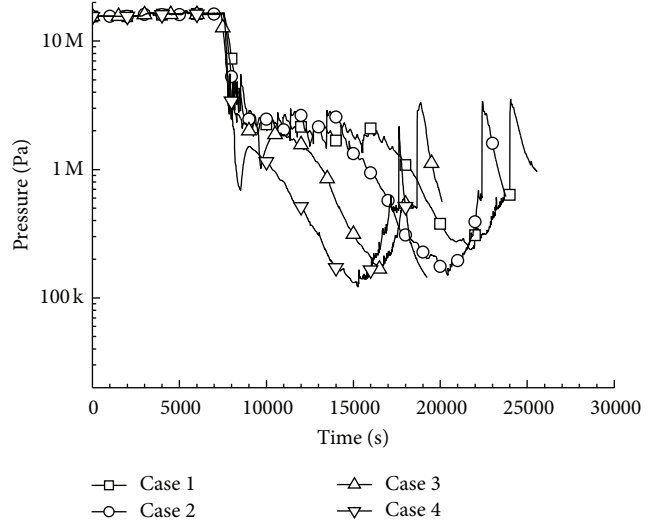


FIGURE 15: RCS pressure with various valve area.

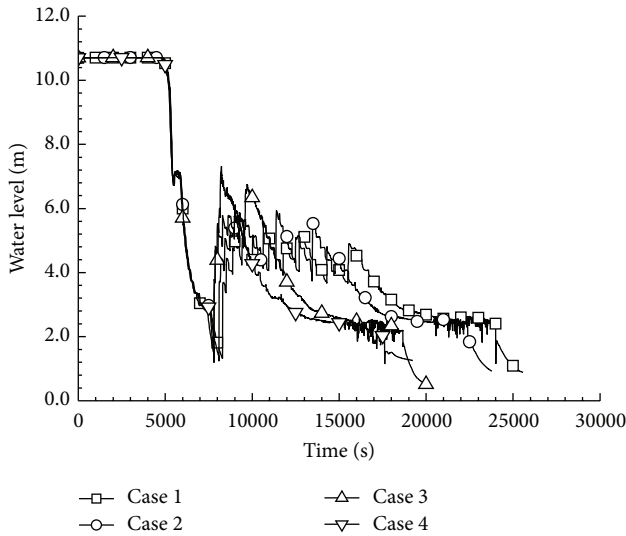


FIGURE 14: Water level of RPV with various valve area.

parametric analysis. The valve area for case 1 is $2.4 \times 10^{-3} \text{ m}^2$; the valve area for case 2 is $3.2 \times 10^{-3} \text{ m}^2$; the valve area for case 3 is $4.8 \times 10^{-3} \text{ m}^2$; the valve area for case 4 is $8.71 \times 10^{-3} \text{ m}^2$. With the increase of valve area, the time of accumulator injection will be earlier and the occurrence of RPV failure will be earlier too (see Figure 14). The high SADV discharge rate which induces excessive loss of water inventory in RCS makes the progression of core degradation to RPV failure faster without additional core cooling water sources. The time of RPV failure is 19240 s for case 1, and it is 6320 s earlier than that for case 4. The water inventory should be used economically for the depressurization strategy. On the other hand, with the decrease of SADV valve area, the RCS pressure reduces more slowly, and the RCS pressure will increase when the lower head of RPV fails (see Figure 15). The RCS pressure is 0.96 MPa for case 1, and it is 0.82 MPa

higher than that for case 4. Furthermore, the SADV discharge rate should make sure that the injection of the cold water from accumulator tanks could take place before the core is severely damaged. It shall avoid accumulator injection after the onset of core melting to limit the hydrogen production. Based on a simplified energy balance equation, an optimum valve area is obtained for Ulchin unit 1 plant, but it needs further analysis and experiment to support the optimization of the valve area [15]. How to optimize the valve area should be further investigated.

5. Conclusions

Chinese improved PWR is modeled using the mechanical analytical code to analyze rapid depressurization capability of SADV. The following conclusions can be drawn from the present work.

- (1) Without activation of the SADV, the RCS pressure is 16.5 MPa which induces large risk of HPME and DCH when lower head of the RPV fails in the three selected severe accidents.
- (2) With activation of the SADV, the RCS pressure is low enough to prevent HPME and DCH in the three selected severe accidents.
- (3) Natural circulation results in heat transfer from the core to the pipes in RCS which may cause the failure of pipes in RCS and delays the accident progression. The creep rupture of pipes in RCS can be avoided by the activation of SADV.
- (4) The introduction of SADV with right valve area will delay progression of core degradation to RPV failure. Valve area is to be optimized since smaller SADV area will reduce its effect and too large valve area will lead to excessive loss of water inventory in RCS and makes core degradation progression to RPV failure faster without additional core cooling water sources.

Highlights

Rapid depressurization capability for Chinese improved PWR is assessed using the mechanical analytical code. Three typical severe accident sequences of TMLB', SBLOCA, and LOFW are selected. Natural circulation at upper RPV and hot leg is considered for the rapid depressurization capacity analysis. Different SADV valve areas are investigated to the influence of depressurization of RCS.

Conflict of Interests

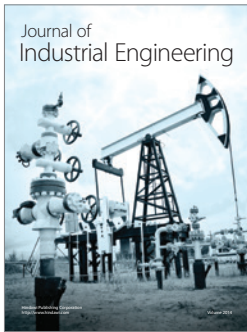
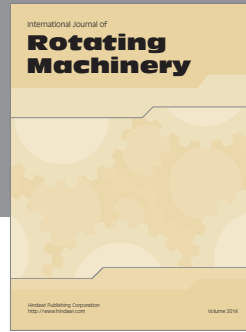
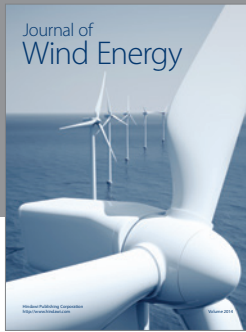
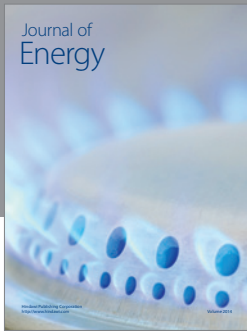
The authors declare that there is no conflict of interests regarding the publication of this paper.

Acknowledgments

This work was supported by the National Natural Science Foundation of China (no. 11205099) and the National Magnetic Confinement Fusion Science Program (no. 2013GB114005).

References

- [1] D. J. Hanson, D. W. Golden, R. Chambers et al., "Depressurization as an accident management strategy to minimize the consequences of direct containment heating," Tech. Rep. NUREG/CR-5447, NRC, Washington, DC, USA, 1990.
- [2] D. A. Brownson, "Intentional depressurization accident management strategy for PWR," Tech. Rep. NUREG/CR-5937, NRC, Washington, DC, USA, 1993.
- [3] J. O. Rodhe, B. W. Morris, and R. A. Bari, "Status of direct containment heating in CSNI member countries: report of task group on ex-vessel thermal-hydraulics," Tech. Rep. NEA/CSNI-153, OECD NEA, Paris, France, 1989.
- [4] U. S. Nuclear Regulatory Commission, "Individual plant examination for severe accident vulnerabilities 10 CFR 50.54 (f). (Generic Letter No. 88-20)," Tech. Rep., NRC, Washington, DC, USA, 1988.
- [5] Y. M. Kwon, H. S. Lim, and J. H. Song, "Design options for safety depressurization system," *Nuclear Engineering and Design*, vol. 179, no. 3, pp. 287–296, 1998.
- [6] R.-J. Park, S.-B. Kim, S.-W. Hong, and H.-D. Kim, "Detailed evaluation of coolant injection into the reactor vessel with RCS depressurization for high pressure sequences," *Nuclear Engineering and Design*, vol. 239, no. 11, pp. 2484–2490, 2009.
- [7] K. Zhang, X. W. Cao, J. Deng et al., "Evaluation of intentional depressurization strategy in Chinese 600 MWe PWR NPP," *Nuclear Engineering and Design*, vol. 238, no. 7, pp. 1720–1727, 2008.
- [8] H. Sjøvall, "Severe accident management in olkiluoto 1 and 2," in *Proceedings of the OECD Workshop on the Implementation of Severe Accident Management Measures*, PSI-Villigen, Switzerland, 2001.
- [9] F. Bouteille, G. Azarian, D. Bittermann, J. Brauns, and J. Eyink, "The EPR overall approach for severe accident mitigation," *Nuclear Engineering and Design*, vol. 236, no. 14–16, pp. 1464–1470, 2006.
- [10] U. S. Nuclear Regulatory Commission, "Individual plant examination for severe accident vulnerabilities 10 CFR 50.54(f)," Tech. Rep., NRC, Washington, DC, USA, 1988.
- [11] L. N. Kmetyk, R. K. Cole, R. C. Smith et al., "MELCOR 1.8.2 assessment: surry PWR TMLB' (with a DCH Study)," Tech. Rep. SAND93-1899, Sandia National Laboratories, Calif, USA, 1994.
- [12] U. S. Nuclear Regulatory Commission, "Severe accident risks: an assessment for five U.S. nuclear power plants," Tech. Rep. UREG-1150, NRC, Washington, DC, USA, 1990.
- [13] W. A. Stewart, A. T. Pieczynski, and V. Srinivas, "Experiments on natural circulation flows in steam generators during severe accidents," in *Proceedings of the International ANS/ENS Topical Meeting on Thermal Reactor Safety*, San Diego, Calif, USA.
- [14] G. M. Martinez, R. J. Gross, M. J. Martinez et al., "Independent review of SCDAP/RELAP 5 natural circulation calculations," Tech. Rep. SAND91-2089, Sandia National Laboratories, 1994.
- [15] C. Huh, N. Suh, and G.-C. Park, "Optimum RCS depressurization strategy for effective severe accident management of station black out accident," *Nuclear Engineering and Design*, vol. 239, no. 11, pp. 2521–2529, 2009.



Hindawi

Submit your manuscripts at
<http://www.hindawi.com>

